Creation of a magnetic plasmon polariton through strong coupling between an artificial magnetic atom and the defect state in a defective multilayer microcavity

D. Y. Lu,[1] H. Liu,[1,][*] T. Li,[1] S. M. Wang,[1] F. M. Wang,[1] S. N. Zhu,[1] and X. Zhang[2]

[1]*Department of Physics, National Laboratory of Solid State Microstructures, Nanjing University,*
Nanjing 210093, People's Republic of China

[2]*5130 Etcheverry Hall, Nanoscale Science and Engineering Center, University of California, Berkeley, California 94720-1740, USA*

We studied the propagation of an electromagnetic (EM) wave in a defective multilayer microcavity with an artificial magnetic atom located at the edge of the defect layer. When the frequency of the defect state is tuned to the resonance frequency of the magnetic atom, strong coupling happens between this atom and EM waves. It creates a type of magnetic plasmon polariton (MPP) with Rabi-type splitting effect that results in the two branches of the MPP mode. The linewidth of the MPP and Rabi-type oscillation of magnetic field inside the atom are investigated in the simulations. A great enhancement of local fields can also be obtained from the MPP, which has a good application in nonlinear optics.

Experimental studies of atom-photon interaction have early been carried out in the field of solid state physics and atomic physics. They are usually realized between atoms or quantum wells and optical media such as photonic crystals[1,2] and cavities.[3–9] A Rabi vacuum-field splitting effect is observed at both the atom-cavity coupling[4,5] and the quantum well–cavity interaction.[9] In recent researches of metamaterials, artificial nanostructures such as nanoparticles and split ring resonators (SRR) have attracted wide study interest. These resonant elements behave like real atoms when they interact with electromagnetic (EM) waves. Their electric or magnetic responses play important roles in the characterization of metamaterials.[10–32] The interaction between nanoparticles and photons has been studied in periodic structures by Linden *et al.*[11] Such a nanoparticle-photon interaction results in selective suppressed extinction of plasmon resonance and, by changing the array period, can be tuned continuously. Similar coupling happens between nanowires and waveguide modes, leading to the formation of a quasiparticle mode with a surprisingly large Rabi splitting.[12]

Up to now, studies of magnetic resonances have been developed in spectra from microwave to visible frequencies.[13–32] Besides SRR,[13–19] "fishnet" structures,[20–23] together with nanowire pairs[24–27] and stacked nanodisks,[28,29] have been invented to work as magnetic resonators in the visible range. Linden *et al.* reported that nanowire pairs, viewed as magnetic atoms, can interact with each other by an adjacent dielectric slab waveguide, giving rise to an avoided crossing at near-infrared wavelengths.[30]

These coupling modes belong to new types of plasmon polaritons that have already inspired a proliferation of experimental and theoretical research work in surface science.[31–33] In our recent paper, another kind of magnetic plasmon polariton (MPP) mode was produced in a linear chain of SRRs, resulting from the strong exchange current interaction between these "magnetic atoms."[34] Meanwhile, this kind of coupled magnetic plasmon can be used to produce optical activity effect.[35]

In this paper, we design a configuration in which one gold nanosandwich, viewed as a magnetic atom, is embedded into a defective multilayer microcavity. Another type of MPP is created by the strong coupling between the atom and the defect mode of EM waves. Rabi-type splitting is observed in this system, which results in the two branches of the MPP. Correspondingly, Rabi-type oscillation is found in the time domain. The change of linewidth of the MPP and its dependence on the position of the atom are also investigated in our simulations. Great local field enhancement is realized in the resonance region of the MPP, which has a good potential application in nonlinear optics.

It is well known that a one-dimensional perfect periodic multilayer possesses a forbidden band gap for the propagation of EM waves. Some allowed modes, so-called defect states, appear inside the band gap when the symmetry of the multilayer is disrupted.[36] In Fig. 1(a), we construct such a one-dimensional multilayer microcavity, which comprises 8-period alternately stacked A-B layers with one defect layer in the middle. Layer A and the defect layer are filled with air ($n_1 = 1.0$) and layer B with a high-refraction material indium tin oxide (ITO, $n_2 = 2.0$). To describe the geometry size of the microcavity, we introduce a cavity parameter ξ. The thickness of A, B, and the defect layer is defined as $d_1 = \xi/(2n_1)$, $d_2 = \xi/(2n_2)$, and $d = \xi/n_1$. For a given value of ξ, a transmission peak is obtained in the band gap for an EM wave at the frequency $\nu = c/(2\xi)$ (c is the speed of light in vacuum), which originates from the presence of a localized defect mode inside the microcavity.

One nanosandwich, composed of two equal-sized gold nanodisks and a middle gap, is located near the edge of the defect layer; the middle gap parallel to the y-z plane is filled with the same material ITO as layer B. Its geometry size is given in Fig. 1(b). Such a nanosandwich acts as an artificial magnetic atom.
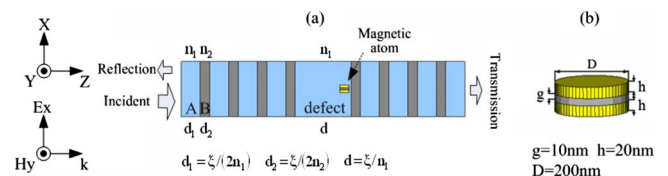

FIG. 1. (Color online) (a) Scheme of a multilayer microcavity with a magnetic atom located at the edge of the defect layer; (b) structure of the magnetic atom.
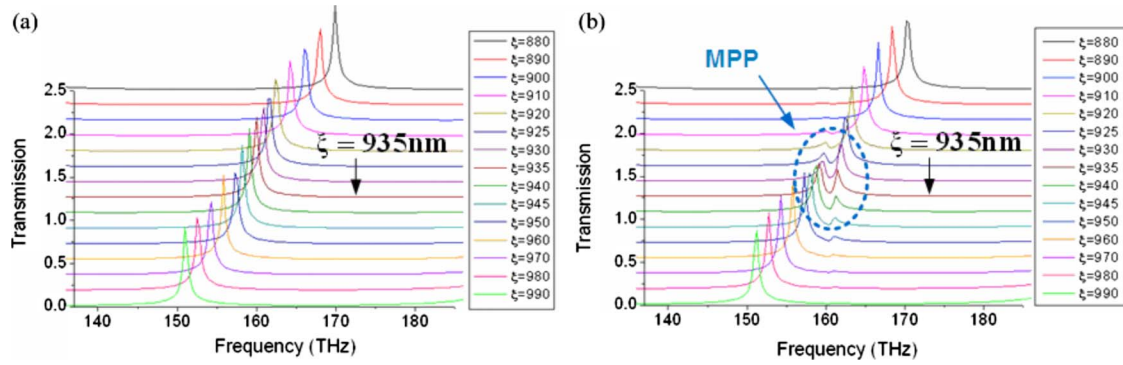
FIG. 2. (Color online) Transmission versus frequency (with cavity parameter ξ from 880 to 990 nm): (a) the results of the microcavity without atom; (b) the results of the microcavity with an atom located at the edge of the defect layer.

To study the propagation property of EM waves in our system, we perform a set of finite-difference time-domain (FDTD) calculations using a commercial software package CST Microwave Studio (Computer Simulation Technology GmbH, Darmstadt, Germany). We rely on the Drude model to characterize the bulk metal properties. Namely, the metal permittivity in the infrared spectral range is given by $\varepsilon(\omega) = 1 - \omega_p^2/(\omega^2 + i\omega\omega_\tau)$, where ω_p is the bulk plasma frequency, and ω_τ is the relaxation rate. For gold, the characteristic frequencies fitted to experimental data are $\omega_p = 1.37 \times 10^4$ THz and $\omega_\tau = 40.84$ THz.[37]

In our simulation setup, a polarized EM wave propagates in the z direction, with its magnetic field in the y direction and electric field in the x direction. As the cavity parameter ξ is tuned from 880 to 990 nm, we perform transmission spectrum calculation of the microcavity without atom [Fig. 2(a)] and with an atom [Fig. 2(b)]. For the microcavity without atom, the transmission peak in the band gap is fixed at the frequency $\nu = c/(2\xi)$ as reported before.[36] For the microcavity with an atom, the transmission peak still observes the rule $\nu = c/(2\xi)$ when ξ is far away from the value 935 nm (outside the blue circle: $\xi > 950$ nm or $\xi < 920$ nm). However, when ξ approaches the value 935 nm (inside the blue circle: 920 nm $\leq \xi \leq 950$ nm), it is surprisingly found that two transmission peaks appear: Drifting away from $\nu = c/(2\xi)$, one peak blueshifts to higher frequency while the other redshifts to lower frequency.

In order to explore the physical origin of these two transmission peaks, a probe is placed inside the magnetic atom to detect the local magnetic field H_y. Variation of $|H_y|$ versus frequency is given in Fig. 3. Under different ξ, there are always two peaks in each curve. When ξ is far away from the value 935 nm (outside the blue circle: $\xi > 950$ nm or $\xi < 920$ nm), one peak changes with ξ according to the rule $\nu = c/(2\xi)$, which obviously comes from the defect mode of the microcavity. The field distribution of this defect mode is shown in Fig. 4. The other peak fixes at the frequency 160.3 THz, which comes from the magnetic resonance of the atom. It does not change with ξ because it is only determined by the geometry structure of the atom. The magnetic resonance mode is very different from the defect mode. It is confined inside the magnetic atom and does not contribute to the propagation property of the whole system. This can explain why the magnetic resonance mode causes a resonant peak in

Fig. 3 but no corresponding transmission peak in Fig. 2(b).

In the foregoing discussions about Fig. 3, we are limited to the results for $\xi > 950$ nm and $\xi < 920$ nm. When ξ is in the range 920 nm $\leq \xi \leq 950$ nm (inside the blue circle), it will be quite different: the defect mode does not comply with the rule $\nu = c/(2\xi)$ anymore, and the magnetic resonance does not keep at 160.3 THz either. As the defect mode is very close to the resonance frequency of the atom, EM energy can be exchanged between these two energy levels. Therefore, strong coupling interaction is established between the defect mode and the magnetic atom. This photon-atom coupling completely changes the characters of EM modes in the microcavity. In the coupling region surrounded by the blue circle, the resonance peaks are neither pure defect mode nor pure magnetic resonance mode. The physical essence of this kind of coupled photon-atom mode is a type of MPP with the two peaks corresponding to its two branches. Basically, the MPP is a kind of a propagation mode that can also transfer EM energy through the system. So, the two transmission peaks surrounded by the blue circle in Fig. 2(b) come from the two branches of this MPP.

To give further evidence of the MPP, its linewidth versus ξ is presented in Fig. 5. The linewidth of the atom is larger than that of the defect state. In the coupling range 920 nm $\leq \xi \leq 950$ nm, the linewidth of two branches of the MPP are between those of the atom and the defect state. As ξ increases, the linewidth of the upper branch of the MPP (de-
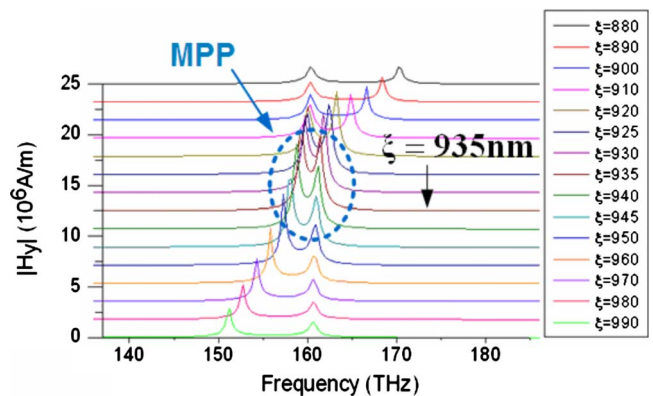

FIG. 3. (Color online) Local field $|H_y|$ detected inside the magnetic atom versus frequency (with cavity parameter ξ from 880 nm to 990 nm).
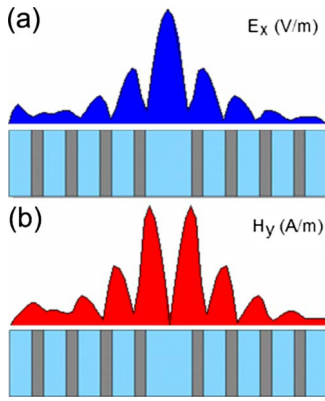
FIG. 4. (Color online) (a) Electric field and (b) magnetic field distribution of the defect state in the microcavity at 170.2 THz with ξ=880 nm.

FIG. 5. (Color online) Linewidth of the resonance peak versus cavity parameter ξ. Black dotted line: lower branch of the MPP; red dotted line: upper branch of the MPP. (Dashed lines represent the resonance linewidth of the atom and the defect state.)

noted as red dotted line) increases from the defect state to the atom state, while the linewidth of the lower branch of the MPP (denoted as black dotted line) decreases from the atom state to the defect state. Therefore, in the coupling region, it is impossible to distinguish between the atom state and the defect state. This linewidth averaging further suggests that the MPP is neither pure atom state nor pure defect state, but a mixed state.

We have already demonstrated that the peak splitting in Fig. 2(b) originates from the coupling effect between the defect mode and the magnetic atom. This phenomenon is extraordinarily similar to the Rabi splitting of energy level of a real atom interacting with EM waves. The two branches of the MPP in Figs. 2(b) and 3 can be seen as the results of Rabi–type splitting of resonance mode of the magnetic atom. To illustrate the splitting effect explicitly, the dependence of the peak frequency of local field $|H_y|$ on the cavity parameter ξ is given in Fig. 6(a). The horizontal and oblique dashed lines represent the resonance frequency of the magnetic atom and the defect state, respectively. They intersect at ξ =935 nm. In the region near the crossing point (inside the blue circle), strong coupling happens and Rabi-type splitting effect is obvious (denoted as red arrow in the figure). Two energy levels are formed in the splitting: One is above the energy level of the atom, which is denoted as the upper branch of the MPP; the other is below the energy level of the atom, which is denoted as the lower branch of the MPP. For example, for ξ=935 nm, the upper level is at 161.5 THz and the lower level at 159.4 THz, thus, the energy gap 2.1 THz is achieved.

So far, the property of the MPP is only studied in the frequency domain. Its behavior in the time domain can also be investigated in our simulations. After being excited by a 5-fs pulse signal, the evolution of magnetic field inside the atom is recorded by the probe, given in Fig. 6(b). For a natural two-level atom, Rabi oscillation could be established when it interacts with a photon.[38] In our system, the nanosandwich could be seen as an artificial two-level atom if the two resonance frequencies of the MPP in the coupling range [encircled by blue curve in Fig. 6(a)] are taken as two energy levels of this magnetic resonator. From Fig. 6(b), it is very interesting that Rabi-type oscillation could also be real-
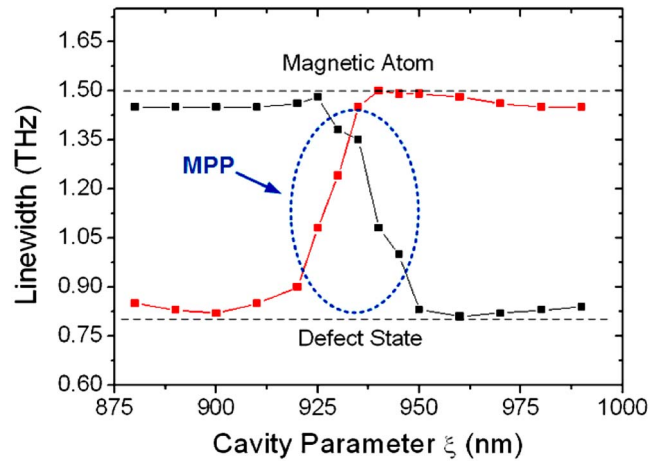
ized in our system. When excited by an EM wave, the stored energy inside the atom is transmitted back and forth between these two energy levels. Therefore, the Rabi-type oscillation is observed in the evolution of local field inside the atom. Meanwhile, its amplitude decays with time due to ohmic loss and radiation loss, with the decay time obtained as 0.8 ps.

Above, we base our discussion on the condition that the atom is placed at the edge of the defect layer. What will happen if we change its position? Actually, the location of the atom plays an important role in the coupling process. When interacting with EM waves, the atom can be viewed as a magnetic dipole $\vec{m}$. The coupling strength is determined by the interaction energy $\Delta E = -\vec{m} \cdot \vec{B}(\vec{r})$, where $\vec{B}(\vec{r})$ is the local magnetic field of the defect mode at the atom. Therefore, to achieve strong coupling, the atom needs to be placed at the location where the magnetic field is enhanced most. From the field distribution of the defect mode given in Fig. 4(b), it is obvious that its magnetic field reaches maximum at the edge and drops to zero at the center of the defect layer. The best choice for the atom is at the edge, which is just what we have already done. Contrarily, if the atom is placed at the center where $\vec{B}(\vec{r})$=0, the interaction term will vanish, which means no coupling interaction happens between the atom and the defect mode. The simulation results in Figs. 6(c) and 6(d) show that Rabi-type splitting effect, as well as Rabi-type oscillation, disappears as estimated. It provides a further confirmation that the MPP proposed in this paper is created completely through the interaction between two modes.

Finally, the MPP is also used to enhance local field in the microcavity. Variation of the magnetic field intensity at the atom versus ξ is shown in Fig. 7. Our system exhibits a much greater local field enhancement when it enters the strong atom-photon coupling than that in the uncoupling region, because, in the coupling range, much more EM energy is absorbed by the atom through the mode interaction, and high energy storage results in the great enhancement. This localization of EM energy by the MPP could serve as a possible application in nonlinear optics.
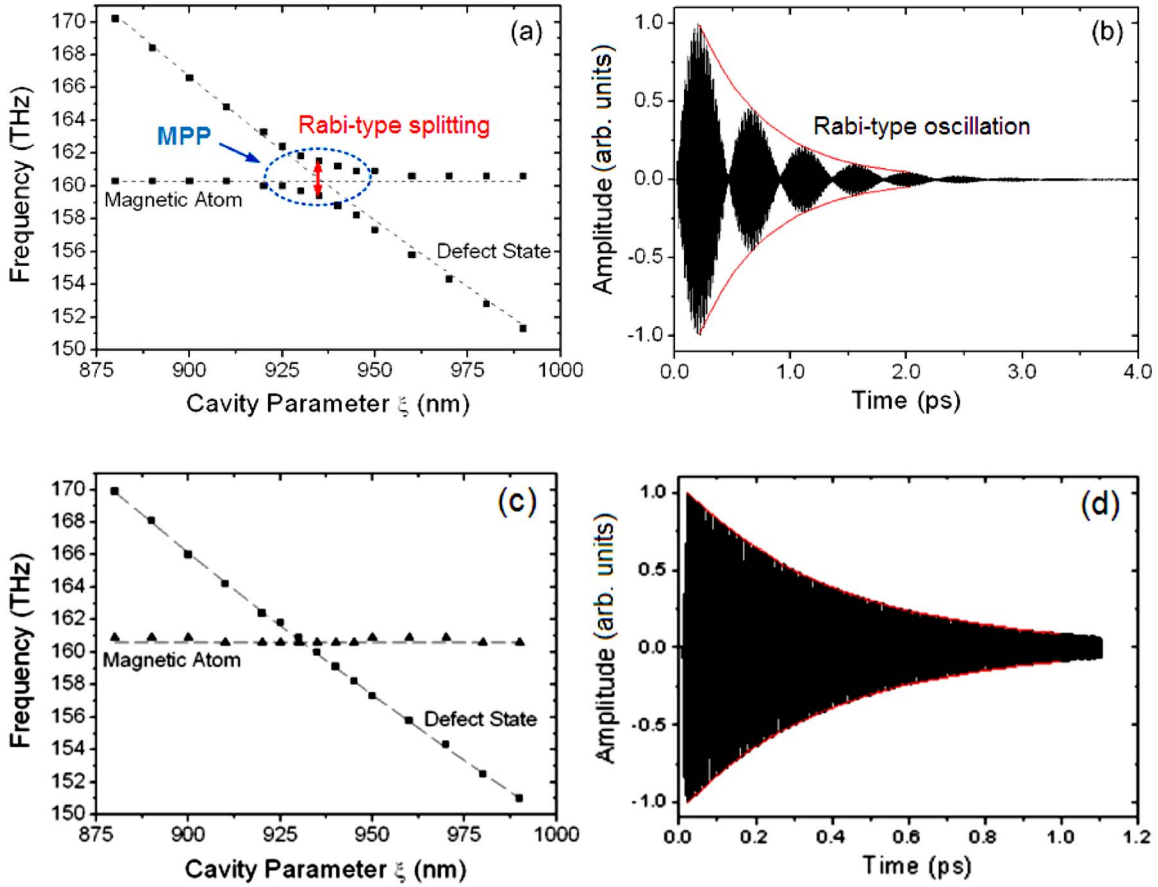
FIG. 6. (Color online) When the atom is located at the edge of the defect layer: (a) the peak frequency of local field $|H_y|$ inside the atom versus cavity parameter ξ; (b) the evolution of magnetic field inside the atom after excited by a 5-fs pulse signal (with $\xi=935$ nm). When the atom is located at the center of the defect layer: (c) the peak frequency of local field $|H_y|$ inside the atom versus cavity parameter ξ; (d) the evolution of magnetic field inside the atom after excited by a 5-fs pulse signal (with $\xi=935$ nm).

In conclusion, we have demonstrated by numerical simulations that a type of MPP is created in a system of an artificial magnetic atom situated within a defective multilayer microcavity in the 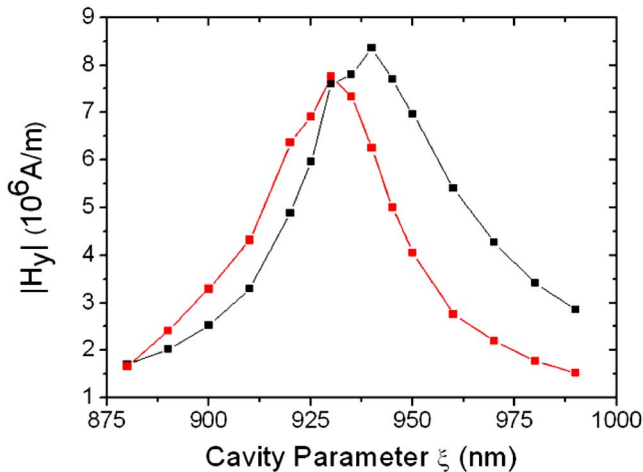same way as a system of real atoms in an optical cavity. Transmission spectrum calculation and local field detecting reveal its Rabi-type splitting and linewidth averaging feature. These effects are attributed to strong coupling between the magnetic atom and the defect mode. The upper and lower normal modes stand for the two branches of the MPP at the coupling region. EM field localization is significantly enhanced as compared to that of the uncoupling or weak coupling, which makes more energy gather in the multilayer microcavity. The dependence of the MPP on the position of the magnetic atom and field distribution in the defect layer has also been discussed.

Our model offers a method to realize strong interaction between a magnetic metamaterial element and EM waves inside the microcavities. Tailoring the light-matter interaction via proper design of the artificial atom and microcavity allows control over such important properties as Rabi-type splitting, field localization, etc. This system will be useful for enhancing nonlinear optical effects such as optical bistability, laser operation, and quantum fluctuation.

FIG. 7. (Color online) Amplitude of local field inside the atom versus cavity parameter ξ. Black dotted line: lower branch of the MPP; red dotted line: upper branch of the MPP.

*Author to whom correspondence should be addressed; liuhui@nju.edu.cn

[1] E. Yablonovitch, Phys. Rev. Lett. **58**, 2059 (1987).

[2] M. Fujita, S. Takahashi, Y. Tanaka, T. Asano, and S. Noda, Science **308**, 1296 (2005).

[3] E. T. Jaynes and F. W. Cummings, Proc. IEEE **51**, 89 (1963).

[4] M. G. Raizen, R. J. Thompson, R. J. Brecha, H. J. Kimble, and H. J. Carmichael, Phys. Rev. Lett. **63**, 240 (1989).

[5] R. J. Thompson, G. Rempe, and H. J. Kimble, Phys. Rev. Lett. **68**, 1132 (1992).

[6] Y. Zhu, D. J. Gauthier, S. E. Morin, Q. Wu, H. J. Carmichael, and T. W. Mossberg, Phys. Rev. Lett. **64**, 2499 (1990).

[7] S. Haroche and D. Kleppner, Phys. Today **42** (1), 24 (1989).

[8] G. Björk, S. Machida, Y. Yamamoto, and K. Igeta, Phys. Rev. A **44**, 669 (1991).

[9] C. Weisbuch, M. Nishioka, A. Ishikawa, and Y. Arakawa, Phys. Rev. Lett. **69**, 3314 (1992).

[10] J. B. Pendry, A. J. Holden, W. J. Stewart, and I. Youngs, Phys. Rev. Lett. **76**, 4773 (1996).

[11] S. Linden, J. Kuhl, and H. Giessen, Phys. Rev. Lett. **86**, 4688 (2001).

[12] A. Christ, S. G. Tikhodeev, N. A. Gippius, J. Kuhl, and H. Giessen, Phys. Rev. Lett. **91**, 183901 (2003).

[13] J. B. Pendry, A. J. Holden, D. J. Robbins, and W. J. Stewart, IEEE Trans. Microwave Theory Tech. **47**, 2075 (1999).

[14] D. R. Smith, W. J. Padilla, D. C. Vier, S. C. Nemat-Nasser, and S. Schultz, Phys. Rev. Lett. **84**, 4184 (2000).

[15] R. A. Shelby, D. R. Smith, and S. Schultz, Science **292**, 77 (2001).

[16] T. J. Yen, W. J. Padilla, N. Fang, D. C. Vier, D. R. Smith, J. B. Pendry, D. N. Basov, and X. Zhang, Science **303**, 1494 (2004).

[17] S. Linden, C. Enrich, M. Wegener, J. F. Zhou, T. Koschny, and C. M. Soukoulis, Science **306**, 1351 (2004).

[18] S. Zhang, W. Fan, B. Minhas, A. Frauenglass, K. Malloy, and S. Brueck, Phys. Rev. Lett. **94**, 037402 (2005).

[19] C. Enrich, M. Wegener, S. Linden, S. Burger, L. Zschiedrich, F. Schmidt, J. F. Zhou, T. Koschny, and C. M. Soukoulis, Phys. Rev. Lett. **95**, 203901 (2005).

[20] S. Zhang, W. Fan, N. C. Panoiu, K. J. Malloy, R. M. Osgood, and S. R. J. Brueck, Phys. Rev. Lett. **95**, 137404 (2005).

[21] G. Dolling, C. Enrich, M. Wegener, C. M. Soukoulis, and S. Linden, Science **312**, 892 (2006).

[22] G. Dolling, M. Wegener, C. M. Soukoulis, and S. Linden, Opt. Lett. **32**, 53 (2007).

[23] T. Li, H. Liu, F. M. Wang, J. Q. Li, Y. Y. Zhu, and S. N. Zhu, Phys. Rev. E **76**, 016606 (2007).

[24] V. M. Shalaev, W. Cai, U. K. Chettiar, H. K. Yuan, A. K. Sarychev, V. P. Dracher, and A. V. Kildishev, Opt. Lett. **30**, 3356 (2005).

[25] V. A. Podolskiy, A. K. Sarychev, and V. M. Shalaev, Opt. Express **11**, 735 (2003).

[26] F. M. Wang, H. Liu, T. Li, Z. G. Dong, S. N. Zhu, and X. Zhang, Phys. Rev. E **75**, 016604 (2007).

[27] F. M. Wang, H. Liu, T. Li, S. N. Zhu, and X. Zhang, Phys. Rev. B **76**, 075110 (2007).

[28] L. Gunnarsson, T. Rindzevicius, J. Prikulis, B. Kasemo, M. Käll, S. Zou, and G. C. Schatz, J. Phys. Chem. B **109**, 1079 (2005).

[29] T. Pakizeh, M. S. Abrishamian, N. Granpayeh, A. Dmitriev, and M. Käll, Opt. Express **14**, 8240 (2006).

[30] S. Linden, M. Decker, and M. Wegener, Phys. Rev. Lett. **97**, 083902 (2006).

[31] A. D. Boardman, *Electromagnetic Surface Modes* (Wiley, New York, 1982).

[32] E. L. Albuquerque and M. G. Cottam, Phys. Rep. **233**, 67 (1993).

[33] M. S. Kushwaha, Surf. Sci. Rep. **41**, 1 (2001).

[34] H. Liu, D. A. Genov, D. M. Wu, Y. M. Liu, J. M. Steele, C. Sun, S. N. Zhu, and X. Zhang, Phys. Rev. Lett. **97**, 243902 (2006).

[35] H. Liu, D. A. Genov, D. M. Wu, Y. M. Liu, Z. W. Liu, C. Sun, S. N. Zhu, and X. Zhang, Phys. Rev. B **76**, 073101 (2007).

[36] B. Shi, Z. M. Jiang, and X. Wang, Opt. Lett. **26**, 1194 (2001).

[37] M. A. Ordal, L. L. Long, R. J. Bell, S. E. Bell, R. R. Bell, R. W. Alexander, Jr., and C. A. Ward, Appl. Opt. **22**, 1099 (1983).

[38] Y. Kaluzny, P. Goy, M. Gross, J. M. Raimond, and S. Haroche, Phys. Rev. Lett. **51**, 1175 (1983).